

Next-to-Leading Order QCD Correction to $e^+e^- \rightarrow J/\psi + \eta_c$ at $\sqrt{s} = 10.6$ GeV

Yu-Jie Zhang ^(a), Ying-Jia Gao ^(a), and Kuang-Ta Chao ^(b,a)

^(a) Department of Physics, Peking University, Beijing 100871, People's Republic of China

^(b) China Center of Advanced Science and Technology (World Laboratory), Beijing 100080, People's Republic of China

One of the most challenging open problems in heavy quarkonium physics is the double charm production in e^+e^- annihilation at B factories. The measured cross section of $e^+e^- \rightarrow J/\psi + \eta_c$ is much larger than leading order (LO) theoretical predictions. With the nonrelativistic QCD factorization formalism, we calculate the next-to-leading order (NLO) QCD correction to this process. Taking all one-loop self-energy, triangle, box, and pentagon diagrams into account, and factoring the Coulomb-singular term into the $c\bar{c}$ bound state wave function, we get an ultraviolet and infrared finite correction to the cross section of $e^+e^- \rightarrow J/\psi + \eta_c$ at $\sqrt{s} = 10.6$ GeV. We find that the NLO QCD correction can substantially enhance the cross section with a K factor (the ratio of NLO to LO) of about 1.8-2.1; hence it greatly reduces the large discrepancy between theory and experiment. With $m_c = 1.4\text{GeV}$ and $\mu = 2m_c$, the NLO cross section is estimated to be 18.9 fb, which reaches to the lower bound of experiment.

PACS numbers: 13.66.Bc, 12.38.Bx, 14.40.Gx

One of the most challenging open problems in heavy quarkonium physics and nonrelativistic QCD (NRQCD) is the double charm production in e^+e^- annihilation at B factories. The inclusive production cross section of J/ψ via double $c\bar{c}$ in $e^+e^- \rightarrow J/\psi c\bar{c}$ at $\sqrt{s} = 10.6\text{GeV}$ measured by Belle Collaboration [1] is about a factor of 5 higher than theoretical predictions including both the color-singlet[2] and color-octet[3] $c\bar{c}$ contributions in the leading order (LO) NRQCD [4]. Even more seriously, the exclusive production cross section of double charmonium in $e^+e^- \rightarrow J/\psi\eta_c$ measured by Belle [1, 5]

$$\sigma[J/\psi + \eta_c] \times B^{\eta_c}[\geq 2] = (25.6 \pm 2.8 \pm 3.4) \text{ fb}, \quad (1)$$

and BaBar[6]

$$\sigma[J/\psi + \eta_c] \times B^{\eta_c}[\geq 2] = (17.6 \pm 2.8_{-2.1}^{+1.5}) \text{ fb}, \quad (2)$$

could be larger than theoretical predictions by an order of magnitude or at least a factor of 5. Here $B^{\eta_c}[\geq 2]$ is the branching fraction for the η_c to decay into at least 2 charged tracks, so Eqs. (1) and (2) give the lower bound for this cross section. Theoretically, treating charmonium as a nonrelativistic $c\bar{c}$ bound state, two independent studies by Braaten and Lee [7] and by Liu, He, and Chao [8] showed that at LO in the QCD coupling constant α_s and the charm quark relative velocity v the cross-section of $e^+e^- \rightarrow J/\psi\eta_c$ at $\sqrt{s} = 10.6\text{GeV}$ is about $3.8 \sim 5.5\text{fb}$ (depending on the used parameters, e.g., the long-distance matrix element, m_c and α_s). In comparison with Eq. (1) or Eq. (2), such a large discrepancy between theory and data may present a challenge to our current understanding of charmonium production based on NRQCD and perturbative QCD.

Some theoretical studies have been suggested in order to resolve this large discrepancy problem. In particular, Bodwin, Braaten, and Lee proposed [9, 10] that processes

proceeding via two virtual photons may be important, and Belle data for $J/\psi + \eta_c$ might essentially include the $J/\psi + J/\psi$ events which were produced via two photons. Brodsky, Goldhaber, and Lee suggested that since the dominant mechanism for charmonium production in e^+e^- annihilation is expected to be the color-singlet process $e^+e^- \rightarrow c\bar{c}gg$, the final states observed by Belle might contain J/ψ and a $M \sim 3\text{GeV}$ spin- J glueball \mathcal{G}_J ($J = 0, 2$) [11]. Motivated by these proposals, Belle presented an updated analysis [12], and ruled out the $J/\psi + J/\psi$ and spin-0 glueball scenarios. Ma and Si studied this process by treating the charm quark as a light quark and using light-cone distribution amplitudes to parameterize nonperturbative effects related to the inner structure of charmonium [13]. Similar approaches were also considered by Bondar and Chernyak [14]. But the enhanced cross section is sensitive to the specific form of quark distributions. Hagiwara, Kou and Qiao obtained a result consistent with Ref.[7] and Ref.[8], and conjectured that higher-order corrections in α_s may be huge [15]. There are also other suggestions to resolve the double charmonium problem, and a comprehensive review on related topics and recent developments in quarkonium physics can be found in Ref. [16].

In order to further clarify this problem, in this paper we present a result for the next to leading order (NLO) QCD correction to the process of $e^+ + e^- \rightarrow J/\psi + \eta_c$. As is known, the NLO QCD corrections are important for quarkonium production in inelastic J/ψ photoproduction[17], in J/ψ plus jet and plus prompt photon associated production in two photon collisions[18], and in gluon fragmentation functions for heavy quarkonium[19].

At LO in α_s , $J/\psi + \eta_c$ can be produced at order $\alpha^2\alpha_s^2$, for which we refer to e.g. Ref [8]. There are four Feynman

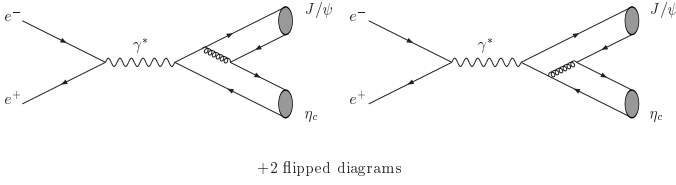


FIG. 1: Born diagrams for $e^-(k_1)e^+(k_2) \rightarrow J/\psi(2p_1)\eta_c(2p_2)$.

diagrams, two of which are shown in Fig. 1, and the other two can be obtained by reversing the arrows on the quark lines. Momenta for the involved particles are assigned as $e^-(k_1)e^+(k_2) \rightarrow J/\psi(2p_1) + \eta_c(2p_2)$. Using the NRQCD factorization formalism, we can write down the scattering amplitude in the nonrelativistic limit to describe the creation of two color-singlet $c\bar{c}$ pairs at short distances, which subsequently hadronize into $J/\psi + \eta_c$ at long distances in the e^+e^- annihilation process. (Note that here the color-octet $c\bar{c}$ contribution is of higher order in v and therefore negligible). Choosing the Feynman gauge, we get the amplitude of Born diagrams

$$i\mathcal{M}_{Born} = \frac{4096\pi e_c \alpha_s m |R_S(0)|^2}{3s^3} \times \epsilon_{\alpha\beta\nu\rho} p_1^\alpha p_2^\beta \varepsilon^{*\nu} \bar{v}_e(k_2) \gamma^\rho u_e(k_1), \quad (3)$$

where $s = (k_1 + k_2)^2$, $e_c = \frac{2}{3}$ is the electric charge of the charm quark, ρ is the Lorentz indices of the virtual photon, ε is the polarization vector of J/ψ . $2p_1$ and $2p_2$ are the momenta of J/ψ and η_c respectively. $R_S(0)$ is the radial wave function at the origin of the ground state charmonium J/ψ and η_c .

At NLO in α_s , the cross section is

$$d\sigma \propto |\mathcal{M}_{Born} + \mathcal{M}_{NLO}|^2 = |\mathcal{M}_{Born}|^2 + 2\text{Re}(\mathcal{M}_{Born}\mathcal{M}_{NLO}^*) + \mathcal{O}(\alpha_s^4). \quad (4)$$

The self-energy and triangle diagrams all correspond to propagators and vertexes of Born diagrams. There remain twenty-four box and pentagon diagrams. Twelve diagrams of them are shown in Fig. 2. The upper $c\bar{c}$ hadronize to J/ψ , and the lower to η_c . The other twelve diagrams are obtained by reversing the arrows on the quark lines. Specially, the associated diagram with Pentagon N12 exists only by reversing the arrows on the lower quark lines which hadronize to η_c .

The self-energy and triangle diagrams are in general ultraviolet (UV) divergent; while the triangle, box, and pentagon diagrams are in general infrared (IR) divergent. Box N5 and N8 and Pentagon N10, which have a virtual gluon line connected with the $c\bar{c}$ in a meson, also contain the Coulomb singularities due to the exchange of longitudinal gluons between c and \bar{c} . In the practical calculation, the IR and UV singularities are regularized with $D = 4 - 2\epsilon$ space-time dimension, and the Coulomb singularities are regularized by a small relative velocity v

between c and \bar{c} [17], $v = |\vec{p}_{1c} - \vec{p}_{1\bar{c}}|/m$, defined in the meson rest frame. For the Coulomb-singular part of the virtual cross section, we find

$$\begin{aligned} \sigma &= |R_S(0)|^4 \hat{\sigma}^{(0)} \left(1 + \frac{2\pi\alpha_s C_F}{v} + \frac{\alpha_s \hat{C}}{\pi} + \mathcal{O}(\alpha_s^2) \right) \\ &\Rightarrow |R_S(0)|^4 \hat{\sigma}^{(0)} \left[1 + \frac{\alpha_s \hat{C}}{\pi} + \mathcal{O}(\alpha_s^2) \right]. \end{aligned} \quad (5)$$

In the second step, the Coulomb-singularity term has to be factored out and mapped into the wave functions of J/ψ and η_c . For the LO expressions of operators $\langle \mathcal{O}^{J/\psi} [{}^3S_1^{(1)}] \rangle$ and $\langle \mathcal{O}^{\eta_c} [{}^1S_0^{(1)}] \rangle$ are associated with $R_S(0)$, and the NLO are proportional to $\pi\alpha_s C_F/v$ [4]. And the two operators give a factor of 2 at $\mathcal{O}(\alpha_s)$, resulting in just the Coulomb-singular term in Eq. (5).

The self-energy and triangle diagrams contain UV singularities, which are removed by the renormalization of the QCD coupling constant g_s , the charm-quark mass m and field ψ , and the gluon field A_μ . Similar to the renormalization scheme in Ref.[18](see also [17]), we define

$$g_s^0 = Z_g g_s, \quad m^0 = Z_m m, \quad \psi^0 = \sqrt{Z_2} \psi, \quad A_\mu^0 = \sqrt{Z_3} A_\mu, \quad (6)$$

where the superscript 0 labels bare quantities and $Z_i = 1 + \delta Z_i$, with $i = g, m, 2, 3$, are renormalization constants. The quantities δZ_i are of $\mathcal{O}(\alpha_s)$ and they contain UV singularities and finite pieces which depend on the choice of renormalization scheme. We define Z_2 and Z_m in the on-mass-shell (OS) scheme, and Z_3 and Z_g in the modified minimal-subtraction ($\overline{\text{MS}}$) scheme

$$\begin{aligned} \delta Z_2^{\text{OS}} &= -C_F \frac{\alpha_s}{4\pi} \left[\frac{1}{\epsilon_{\text{UV}}} + \frac{2}{\epsilon_{\text{IR}}} - 3\gamma_E + 3 \ln \frac{4\pi\mu^2}{m^2} + 4 \right], \\ \delta Z_m^{\text{OS}} &= -3C_F \frac{\alpha_s}{4\pi} \left[\frac{1}{\epsilon_{\text{UV}}} - \gamma_E + \ln \frac{4\pi\mu^2}{m^2} + \frac{4}{3} \right], \\ \delta Z_3^{\overline{\text{MS}}} &= \frac{\alpha_s}{4\pi} (\beta_0 - 2C_A) \left[\frac{1}{\epsilon_{\text{UV}}} - \gamma_E + \ln(4\pi) \right], \\ \delta Z_g^{\overline{\text{MS}}} &= -\frac{\beta_0}{2} \frac{\alpha_s}{4\pi} \left[\frac{1}{\epsilon_{\text{UV}}} - \gamma_E + \ln(4\pi) \right], \end{aligned} \quad (7)$$

where μ is the renormalization scale, γ_E is the Euler's constant and $\beta_0 = (11/3)C_A - (4/3)T_F n_f$ is the one-loop coefficient of the QCD beta function, and n_f is the number of active quark flavors. There are three massless light quarks u, d, s and one heavy quark c , so $n_f = 4$. Color factors are given by $T_F = 1/2$, $C_F = 4/3$, $C_A = 3$ in $SU(3)_c$. Differing from Ref.[18], we take the $\overline{\text{MS}}$ scheme for Z_3 with no external gluon legs and set $n_f = 4$. In this scheme, we do not need to calculate the self-energy on external quark legs. It turned out that the difference for the calculated cross section in different schemes is of order of next to next to leading order and can therefore be neglected in the NLO result. In the NLO corrections we should use the two-loop formula for $\alpha_s(\mu)$,

$$\frac{\alpha_s(\mu)}{4\pi} = \frac{1}{\beta_0 L} - \frac{\beta_1 \ln L}{\beta_0^3 L^2}, \quad (8)$$

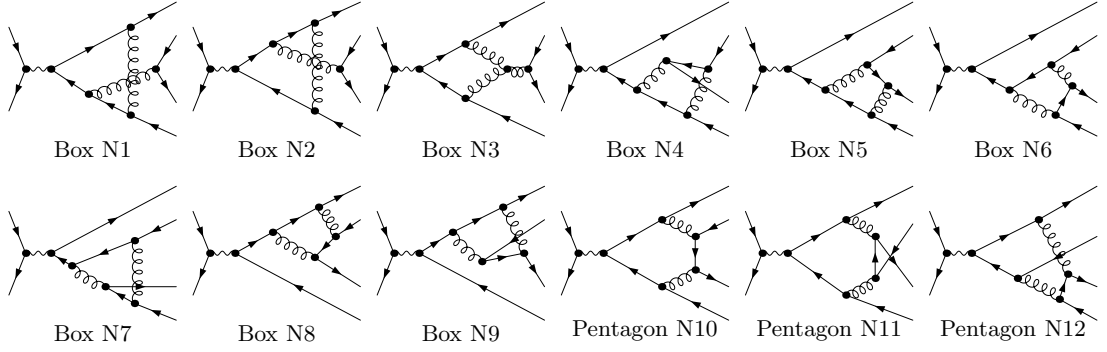


FIG. 2: Twelve of the twenty-four box and pentagon diagrams for $e^-(k_1)e^+(k_2) \rightarrow J/\psi(2p_1)\eta_c(2p_2)$.

where $L = \ln(\mu^2/\Lambda_{\text{QCD}}^2)$, and $\beta_1 = (34/3)C_A^2 - 4C_F T_F n_f - (20/3)C_A T_F n_f$ is the two-loop coefficient of the QCD beta function.

Pentagon diagrams N11 and N12 can be reduced to integrals with a lower number of external legs directly, since there are only two independent momenta. Then they can

be calculated the same way as box diagrams. To treat Pentagon N10 in Fig. 2, we need to calculate the five-point function $E_0[p_1, 2p_1, -p_2, -2p_2, m, 0, m, 0, m]$, and the finite term E_0^{fin} , where

$$\begin{aligned}
 E_0 &= E_0^{fin} + \frac{2}{s} D_0[-p_1, -p_1 - p_2, p_1, 0, m, 0, m] + \frac{2}{s} D_0[p_2, p_1 + p_2, -p_2, 0, m, 0, m], \\
 E_0^{fin} &= \frac{-4}{s} D_0[p_1 + p_2, p_1 + 2p_2, -p_1, 0, 0, m, m] + \int \frac{d^D q}{(2\pi)^D} \frac{2/s(s/2 - 4q \cdot p_1 + 4q \cdot p_2 - 8m^2)}{(q^2 - m^2)(q + p_1)^2((q + 2p_1)^2 - m^2)(q - p_2)^2((q - 2p_2)^2 - m^2)} \\
 &= \frac{2\sqrt{4m^2 - s} \tan^{-1} \frac{\sqrt{s}}{\sqrt{4m^2 - s}} - \sqrt{s} \ln(\frac{-s}{m^2})}{-i\pi^2 m^2 s^{5/2}} + \frac{2(4m^2 - s)^{3/2} \tan^{-1} \frac{\sqrt{s}}{\sqrt{4m^2 - s}} + \sqrt{s} (i\pi(3m^2 - s) + (s - 4m^2) \ln(\frac{-s}{m^2}))}{8im^4 \pi^2 (4m^2 - s) s^{5/2} (16m^2 - s)^{-1}},
 \end{aligned} \tag{9}$$

where the IR- and Coulomb-finite term E_0^{fin} is calculated with dimension $D = 4$ and velocity $v = 0$, and $\ln(-s/m^2) = \ln(-(s + i0)/m^2) = \ln(s/m^2) - i\pi$. In Eq. (9) the $D_0[-p_1, -p_1 - p_2, p_1, 0, m, 0, m]$ term is,

$$D_0 = \frac{4}{s} C_0[-p_1, p_1, 0, m, m] + \frac{i}{(4\pi)^2} \frac{2i\pi - 2\ln 4}{m^2 s}. \tag{11}$$

This term will appear in Box N5, N8. The other IR-divergence terms can be calculated like that. Then all the IR-divergence terms become $C_0[p_1, -p_2, 0, m, m]$ and $C_0[p_{1c}, -p_{1\bar{c}}, 0, m, m]$. We find that Box N3, N6, N7 and Pentagon N12 are IR-finite respectively, and sum of Box N1 + N2 + N4 + N9 is IR-finite, and IR-divergence term of Pentagon N11 is canceled by vertex diagrams. IR-divergence and Coulomb-singular terms of Box N5 + N8 and Pentagon N10 are all related to the $C_0[p_{1c}, -p_{1\bar{c}}, 0, m, m]$ term. With $v = |\vec{p}_{1c} - \vec{p}_{1\bar{c}}|/m \rightarrow 0$,

$$C_0 = \frac{-i}{2m^2 (4\pi)^2} \left(\frac{4\pi\mu^2}{m^2} \right)^\epsilon \Gamma(1 + \epsilon) \left[\frac{1}{\epsilon} + \frac{\pi^2}{v} - 2 \right]. \tag{12}$$

IR-divergence terms of Box N5 + N8 + Pentagon N10 are

canceled by counter terms, and the Coulomb singularity is mapped into $R_S(0)$. UV term is canceled by counter terms. Then the final NLO result for the cross section is UV-, IR-, and Coulomb-finite. Details of the calculation can be found in a forthcoming paper.

We now turn into numerical calculations for the cross section of $e^+ + e^- \rightarrow J/\psi + \eta_c$. To be consistent with the NLO result the value of the wave function squared at the origin should be extracted from the leptonic width at NLO of α_s (see e.g. [4]): $|R_S(0)|^2 = [(9m_{J/\psi}^2)/(16\alpha^2(1 - 4C_F\alpha_s/\pi))]\Gamma(J/\psi \rightarrow e^+e^-)$. Using the experimental value $5.40 \pm 0.15 \pm 0.07$ KeV [20], we obtain $|R_S(0)|^2 = 0.978\text{GeV}^3$, which is a factor of 1.21 larger than 0.810GeV^3 that was used in Refs.[7, 8] from potential model calculations. Taking $m_{J/\psi} = m_{\eta_c} = 2m$ (in the nonrelativistic limit), $m = 1.5$ GeV, $\Lambda_{\overline{\text{MS}}}^{(4)} = 338\text{MeV}$, with Eq.(8) we find $\alpha_s(\mu) = 0.259$ for $\mu = 2m$ (these are the same as in Ref.[8], except here a larger $|R_S(0)|^2$ is used), and get the cross section in NLO

$$\sigma(e^+ + e^- \rightarrow J/\psi + \eta_c) = 15.7\text{fb}, \tag{13}$$

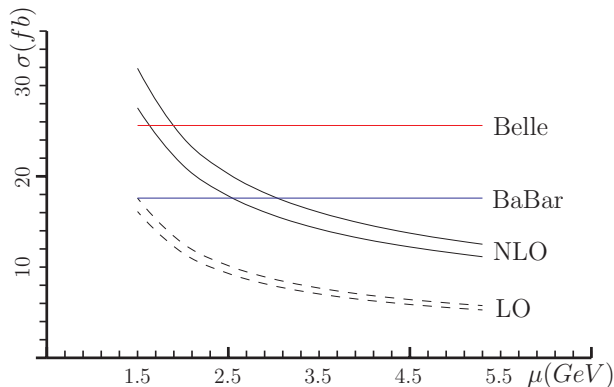


FIG. 3: Cross sections as functions of the renormalization scale μ . Here $|R_S(0)|^2 = 0.978\text{GeV}^3$, $\Lambda = 0.338\text{GeV}$, $\sqrt{s} = 10.6\text{GeV}$; NLO results are represented by solid lines and LO one by dashed lines; the upper line is for $m = 1.4\text{GeV}$ and the corresponding lower line is for $m = 1.5\text{GeV}$; the upper straight line denotes the central value measured by Belle in Eq.(1) and the lower straight line by BaBar in Eq.(2).

which is a factor of 1.96 larger than the LO cross section 8.0 fb. If we set $\mu = m$ and $\mu = \sqrt{s}/2$, then $\alpha_s = 0.369$ and 0.211 , which result in the cross section 27.5 and 11.2 fb respectively. If we set $m = 1.4\text{GeV}$ and $\mu = 2m$, the cross section is 18.9 fb and 9.2 fb at NLO and LO respectively. (Our LO result is also consistent with Ref.[7] if we take their smaller value for $|R_S(0)|^2$ and $\mu = \sqrt{s}/2$.) In Fig. 3 we show the calculated $e^+ + e^- \rightarrow J/\psi + \eta_c$ cross sections at LO and NLO as functions of the renormalization scale μ with two mass values $m_c = 1.4\text{ GeV}$ and 1.5 GeV , as compared with the Belle and BaBar data. We see the NLO QCD correction enhances the cross section by about a factor of 2, despite of existing theoretical uncertainties.

The relativistic corrections may further significantly enhance the cross section[21] (see also [7]). The reason for the enhancement is quite obvious that in Fig. 1 the virtuality of the gluon takes its maximum value of $Q^2 = s/4$ in the nonrelativistic limit, and taking account of the relative momentum between the charm quarks in the charmonium will lower the value of the gluon virtuality.

In conclusion, we find that by taking all one-loop self energy, triangle, box, and pentagon diagrams into account, and factoring the Coulomb singular term associated with the exchange of longitudinal gluons between c and \bar{c} into the $c\bar{c}$ bound state wave function, we get an ultraviolet (UV) and infrared (IR) finite correction to the cross section of $e^+e^- \rightarrow J/\psi + \eta_c$ at $\sqrt{s} = 10.6\text{ GeV}$, and that the NLO QCD correction can substantially enhance the cross section with a K factor (the ratio of NLO to LO) of about 1.8-2.1; and hence it crucially reduces the large discrepancy between theory and experiment. With

$m = 1.4\text{GeV}$ and $\mu = 2m$, the NLO cross section is estimated to be 18.9 fb, which reaches to the lower bound of experiment.

We would like to thank G.T. Bodwin, B.A. Kniehl and J. Lee for helpful comments and discussions. We also thank K.Y. Liu and C. Meng for valuable discussions. This work was supported in part by the National Natural Science Foundation of China (No 10421503), the Key Grant Project of Chinese Ministry of Education (No 305001), and the Research Found for Doctorial Program of Higher Education of China.

-
- [1] K. Abe *et al.* [Belle Collaboration], Phys. Rev. Lett. **89**, 142001 (2002).
 - [2] P. Cho and A.K. Leibovich, Phys. Rev. **D 54**, 6690 (1996); F.Yuan, C.F. Qiao, and K.T. Chao, Phys. Rev. **D 56**, 321 (1997); *ibid*, 1663 (1997); S. Baek, P. Ko, J. Lee, and H.S. Song, J. Korean Phys. Soc. **33**, 97 (1998); V.V. Kiselev *et al.*, Phys. Lett. **B332**, 411 (1994); K.Y.Liu, Z.G.He, and K.T.Chao, Phys. Rev. **D 68**, 031501(R)(2003).
 - [3] K.Y. Liu, Z.G. He and K.T. Chao, Phys. Rev. **D69**, 094027 (2004).
 - [4] G. T. Bodwin, E. Braaten, and G. P. Lepage, Phys. Rev. **D 51**, 1125 (1995); **55**, 5853(E) (1997).
 - [5] P. Pakhlov, hep-ex/0412041.
 - [6] B. Aubert *et al.*[BaBar Collaboration], Phys. Rev. **D 72**, 031101 (2005) .
 - [7] E. Braaten and J. Lee, Phys. Rev. **D 67**, 054007 (2003); **D 72**, 099901(E) (2005).
 - [8] K. Y. Liu, Z. G. He and K. T. Chao, Phys. Lett. **B 557**, 45 (2003).
 - [9] G. T. Bodwin, J. Lee and E. Braaten, Phys. Rev. Lett. **90**, 162001 (2003).
 - [10] G. T. Bodwin, J. Lee, and E. Braaten, Phys. Rev. **D 67**, 054023 (2003).
 - [11] S. J. Brodsky, A. S. Goldhaber and J. Lee, Phys. Rev. Lett. **91**, 112001 (2003).
 - [12] K. Abe *et al.*,(Belle Collaboration), Phys.Rev. **D70** (2004) 071102.
 - [13] J.P. Ma and Z.G. Si, Phys.Rev. **D70** (2004) 074007.
 - [14] A.E. Bondar and V.L. Chernyak, Phys. Lett. **B612**, 215 (2005).
 - [15] K. Hagiwara, E. Kou and C. F. Qiao, Phys. Lett. **B 570**, 39 (2003).
 - [16] N. Brambilla *et al.*, hep-ph/0412158.
 - [17] M. Krämer, Nucl. Phys. **B 459** (1996) 3.
 - [18] M. Klasen, B.A. Kniehl, L.N. Mihaila, and M. Steinhauser, Nucl. Phys. **B713** (2005) 487; Phys. Rev. **D71** (2005) 014016.
 - [19] E. Braaten and J. Lee, Nucl. Phys. **B586** (2000) 427.
 - [20] S.Eidelman, *et al.* [Particle Data Group], Phys. Lett. **B 592** (2004) 1.
 - [21] Z.G. He, Y. Fan, and K.T. Chao, to be submitted.